An infiltration column to investigate experimentally the response of the Soil-Plant-Atmosphere Continuum

R. Dainese
Department of Civil and Environmental Engineering, University of Strathclyde, Glasgow, UK
CIRAD – UMR AMAP & Université de Montpellier, Montpellier, France

A. Belli
Faculty of Engineering, Politecnico di Torino, Torino, Italy

T. Fourcaud
CIRAD – UMR AMAP, Montpellier, France

A. Tarantino
Department of Civil and Environmental Engineering, University of Strathclyde, Glasgow, UK

ABSTRACT: This paper presents an experimental setup to study the SPAC (Soil-Plant-Atmosphere Continuum) and the mechanisms of water extraction by vegetation. The infiltration column was equipped with TDR probes and High-Capacity Tensiometers to monitor the profiles of volumetric water content and suction respectively. A balance was used to monitor the evaporation/evapotranspiration rate. Experiments were run in parallel on a bare sample and a soil sample vegetated with grass respectively. Two different evaporation/evapotranspiration regimes were imposed by considering natural and forced ventilation. The experimental setup was able to capture the transition from the energy-limited to the water–limited regime. The profiles of water content and suction recorded by TDR probes and the high-capacity tensiometers where coherent with the different stages in the evapotranspiration process. The response of the TDR probes has also been successfully validated by comparison with measurements of water content by oven-drying.

1 INTRODUCTION

Vegetation plays an important 'hydrological' role in the stabilization of geostructures.
Water extracted through the root system by transpiration increases the negative pore-water pressure (Garg et al.(2015)) and the plant-induced suction decreases the soil permeability, impeding rainfall infiltration(Ng and Menzies(2007)). This double-effect of increasing and retaining soil suction due to the presence of vegetation has an effect on the mechanical response of the ground (Fredlund et al.(1978); Simon and Collison (2002); Pollen-Bankhead and Simon(2010)).

The formulation of a model to predict the suction profile within the soil due to the presence of vegetation would be a first step towards the application of vegetation for soil stabilization.

A key aspect is the definition of an outward water flux associated with the vegetation, i.e. the hydraulic boundary condition of the geotechnical system. Because the soil and the plant form a continuum with the atmosphere (SPAC – Soil-Plant-Atmosphere Continuum), the characterisation of the hydraulic boundary condition requires an understanding of the interplay between these three components.

This paper presents an experimental setup aimed at investigating the 'continuum' response of silty soil vegetated with grass and the influence on the outward water flux. The soil is monitored using TDR probes and high-capacity tensiometers to measure volumetric water content and matric suction respectively. Atmospheric conditions are varied in terms of relative humidity and air velocity. Transpiration is measured via a balance. Preliminary results are presented in the paper to demonstrate the coherence of the measurements and the effect of vegetation on the hydraulic response of the soil.

2 BACKGROUND

Evapotranspiration (ET) can occur in two different regimes, which are referred to as 'energy-limited' and 'water-limited'.

In the energy-limited regime, evapotranspiration is controlled by the evaporative demand of the atmosphere, which is in turn controlled by the solar radiation and the air relative humidity. Evapotranspiration occurs at its maximum rate and is referred to as Potential Evapotranspiration (PET).

In the water-limited regime, the soil-plant hydraulic system is not able to accommodate the evaporative demand of the atmosphere and the Actual Evapotranspiration (AET) is lower than the potential evapotranspiration ($AET < PET$). The drop in actual evapotranspiration with respect to the potential evapotranspiration depends on the hydraulic response of the soil-plant hydraulic system.

Potential evapotranspiration in the energy-limited regime can be expressed by the Penman-Monteith equation (Monteith 1965):

$$PET = \frac{1}{L[T(z)]}\left[\frac{\Delta \cdot R_n + \rho_a c_p p_{v0}(z)[1-RH\ ]/r_a}{\left[\Delta+\gamma\ \left(\frac{r_a+r_c}{r_a}\right)\right]}\right] \quad (1)$$

where L [J kg^{-1}] is the latent heat of vaporisation of water at the air temperature T(z), PET [kg m^{-2} s^{-1}] the potential evapotranspiration rate, Δ [Pa °C^{-1}] the slope of the saturation vapour pressure curve at the air temperature T(z), γ [Pa °C^{-1}] the psychrometric constant at the air temperature T(z), R_n [W m^{-2}] the rate of net radiation, ρ_a the air density [kg m^{-3}], c_p [J kg^{-1} °C^{-1}] the specific heat of air, p_{v0} [Pa] the saturation vapour pressure at the air temperature T at the elevation z, RH the relative humidity at the elevation z, r_a [s m^{-1}] the resistance term for the aerial transport of water vapour from the canopy, r_c [s m^{-1}] the canopy resistance (resistance at the leaf level of the transpiring crop).

The aerodynamic resistance r_a is a function of the wind velocity and surface roughness. As an example, the following empirical equation was proposed by Penman (1956) for mown grass:

$$r_a = \frac{250}{0.5 + 0.54 \cdot v_x(z=2m)} \quad \left[\frac{s}{m}\right] \quad (2)$$

where v_x [m s^{-1}] is the wind velocity at 2m height.

3 MATERIALS AND METHODS

3.1 *Experimental setup*

Two cylindrical columns were implemented, the first one to accommodate a sample vegetated with grass and a second one left bare to operate as a control (Figure 1). Holes were machined through the wall to install High-Capacity Tensiometers (HCT) and Time Domain Reflectometry (TDR) probes to monitor the evolution of suction and water content respectively at different depths (Table 1). The evaporation rate (bare soil) and the evapo-transpiration rate (vegetated soil) were monitored by placing each column on a balance. Column dimensions and instruments location are indicated in Table 1.

Table 1: Column dimension and instrument location

Column dimension	
Inner diameter [mm]	295
Inner height [mm]	250
Wall thickness [mm]	9
Instruments location (from top)	
1st level (1 TDR- 1 HCT) [mm]	40
2nd level (2 TDR – 1 HCT) [mm]	125
3rd level (1 TDR – 1 HCT) [mm]	210

The bottom part of the columns was equipped with a filter, composed of two layers of geotextile and an intermediate layer of coarse sand and gravel. The system was connected to a water reservoir (Figure 1) to impose an initial hydrostatic pore-water pressure distribution associated with a water table at the same level as the top surface of the sample.

Figure 1. Imposing an initial hydrostatic pore-water pressure distribution, through connection to a water reservoir (water table at the specimen surface level).

3.2 *Soil and sample preparation*

The soil was 'designed' to be a well-graded material with an air entry value of at least a few tenths of kPa and a gradual transition from the saturated to the residual state. It was obtained by mixing different soils as shown in Table 2. The index properties of the mix are also reported in Table 2.

Table 2: Soil mix composition and index properties

Soil mix composition	
CH30 [%]	36
Sand 2: CN HST 95 [%]	24
Silt: Ventilated quartz [%]	35
Clay: Kaolin [%]	5
Grain size distribution	
Sand content (≤ 2 mm, %)	60
Silt content (≤ 63 μm, %)	35
Clay content (≤ 2 μm, %)	5
Specific gravity	2.64

An initial attempt was made to prepare the sample from slurry state and consolidate it by inducing evaporation at its surface. However, the soil showed tendency to segregate and the final density was too high for the herbage to develop a root system.

The sample was therefore prepared by compaction. The four soils were mixed dry and the powder was wetted by spraying an amount of water equal to 24% of the mass of clay and silt (9.6% of the total mass of soil). The moistened powder was gently mixed, placed in the column, and compacted to 100 kPa vertical stress to obtain a dry density ρ_d=1.85 g/cm^3.

The two columns were then connected to the water reservoir and the water table was imposed at the specimen surface level (Figure 1). The valve connecting the reservoir to the column was then closed and the samples were let dry for 7 days. At this stage

the soil was stiff enough to drill a hole approximately 2mm diameter to insert the seeds into the sample.

The columns were placed in a laboratory environment at a controlled temperature (20°C) and reltive humidity (RH=45%). The solar radiation was simulated using a 36 W growth lamp, with a daily cycle of 14 hours of light and 10 h of darkness.

3.3 *Grass species and growth conditions*

The selected vegetation was *Lolium Perenne*, a grass species from the family of *Poaceae*. The plant is commonly used in Europe for slope stabilisation and erosion protection due to its ability to germinate easily. The herbaceous species was chosen for its fast growth as it typically germinates within 4-5 days from sowing. In order to obtain a relevant root density, 3 seeds were inserted in each 1-cm deep-hole, for a horizontal grid of 1 cm spacing in two orthogonal directions. The soil was kept moistened to allow the grass to grow. It was irrigated by capillarity by positioning the level of the water reservoir in correspondence to the bottom surface of the two samples.

3.4 *HCT and TDR: conditioning*

High-Capacity Tensiometers were pre-pressurised at 4MPa before use and cycles of cavitation and pre-pressurisation were applied to improve the performance of the tensiometer in terms of maximum sustainable suction and measurement duration (Tarantino (2004)). After removal from the saturation chamber, the tensiometers were placed in free water for zeroing. A kaolin paste –approximately at the plastic limit –was applied on the tensiometer porous filter to ensure proper hydraulic continuity with the soil. The loss of water from the soil is a slow process, the thin layer (few millimetres) of kaolin paste is then capable of transferring the water tension to the HCT with no appreciable delay—after the time interval necessary to reach a hydraulic equilibrium with the specimen (in the range of few hours).

Each TDR probe was calibrated for travel time and electric length by performing measurements in air and demineralized water according to Tarantino et al. (2008). The apparent permittivity K_a was related to the soil volumetric water content according to the equation proposed by Ledieu et al. (1986):

$$\theta = 0.1138 \cdot \sqrt{K_a} - 0.1758 \qquad (3)$$

where Ka is the apparent dielectric permittivity inferred from the velocity of propagation of the electromagnetic wave through the probe.

3.5 *Experimental procedure*

After 15 days from sowing, the column was disconnected from the water reservoir and the excess of water was let leak through the bottom drain; the drain was then close. The water was let evaporate from the top surface of the soil in the two columns. Monitoring started 28 days after the grass was seeded, which corresponds to Day 0 of the test. Data were recorded for 29 days to track the water content and pore-water pressure profiles developing in the column due to the water loss induced by the evaporation/evapo-transpiration process. The two columns were subjected to the boundary conditions described in Table 3. From day 0 to day 19, the surface of the samples was exposed to natural ventilation. On day 19, a forced ventilation was imposed at the surface level of the two columns in order to increase the evaporation rate and possibly bring the sample into the water-limited regime.

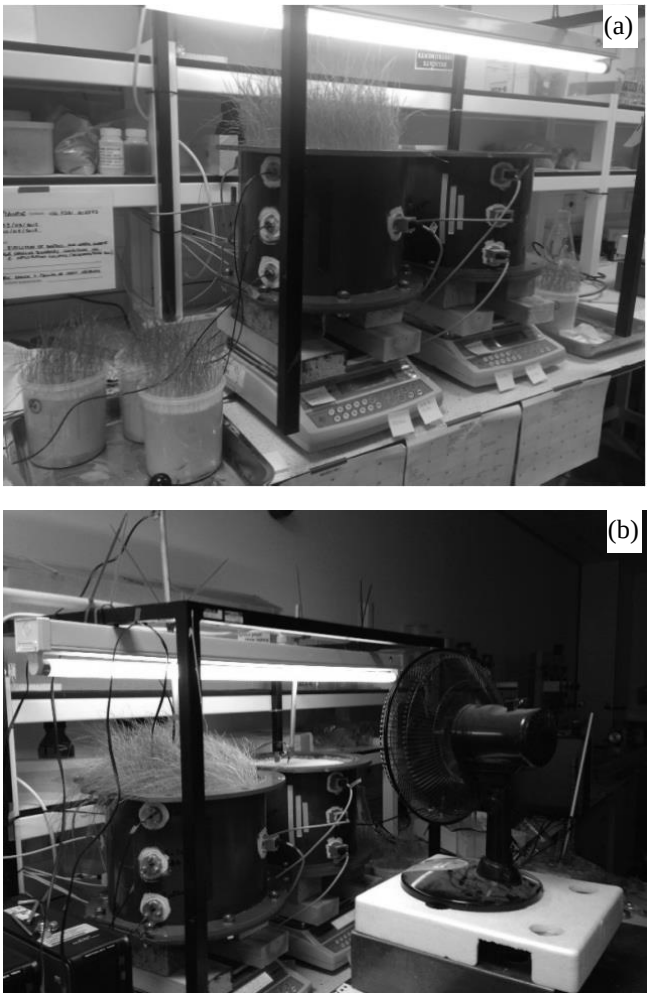

Figure 2. Boundary conditions imposed (a) BC1 – natural ventilation (b) BC2 - forced ventilation

Table 3. 'Atmospheric' Boundary Conditions during the test

Stage	BC1	BC2
Time interval (days)	0-18	19-24
Forced ventilation (fan)	No	Yes
Daily cycle:		
Growth lamp (h)	14	14
Darkness (h)	10	10
Environmental conditions:		
Temperature (°C)	20°C	20°C
Relative humidity (%)	~45 %	~45 %

4 RESULTS AND DISCUSSION

Outward water flux was derived from the measurement of column weight recorded continuously by the balance. Figure 3 shows the water loss in terms of average volumetric water content θ_{av} for the bare and vegetated column respectively calculated using Eq. (4):

$$\theta_{average} = \frac{V_w}{V_{tot}} = \theta_{average,fin} + \frac{\Delta m/\rho_w}{V_{tot}} \quad (4)$$

where V_w is the volume of water in the sample, V_{tot} is the total volume of the sample, $\theta_{av,fin}$ is the average volumetric water content of the sample at the end of the test, Δm [g] is the cumulative change in mass with respect to the mass of the column at the end of the end of the test, and ρ_w is the density of water.

The value of the final average volumetric water content for each column was calculated from the average of the volumetric water content measured on samples collected from around the TDR probes at the end of the test (Table 4).

Table 4. Local and average volumetric water contents and total mass at the end of the test

	Probe	$\theta_{loc,final}$	$\theta_{av,final}$	V_{tot} [m^3]	m_{final} [kg]
Vegetated Column	TDR 1	0.028	0.037	0.066	35.14
	TDR 2	0.041			
	TDR 3	0.043			
Bare Column	TDR 6	0.026	0.041	0.066	35.71
	TDR 7	0.048			
	TDR 8	0.050			

Figure 3 shows the changes in average volumetric water content for the two columns for the whole duration of the test. Measurements were taken under two sets of boundary conditions, i.e. BC1 (natural ventilation) and BC2 (forced ventilation).

Figure 4 report the rates of daily evaporation and evapotranspiration obtained by dividing the flow rate by the surface area of the sample (Ø=29.5 cm).

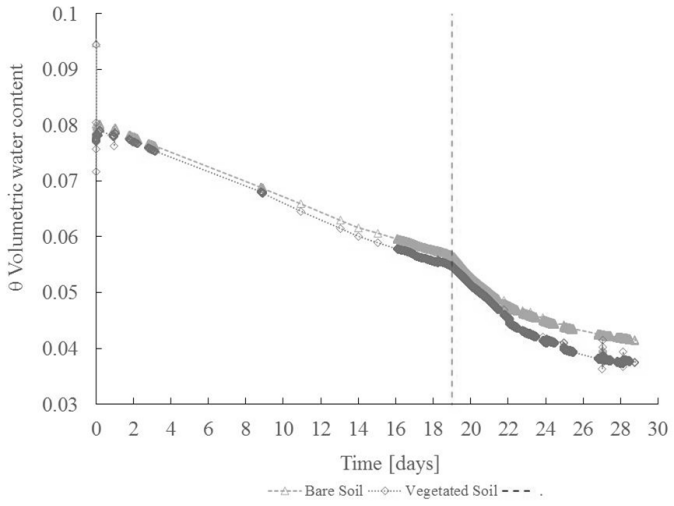

Figure 3: Volumetric water content over time for vegetated and bare soil

BC1 corresponds to the condition of natural ventilation. Evaporation/evapotranspiration appears to be similar for the bare and vegetated surfaces (Table 5). There are two possible explanations for this response. Let us rewrite the Penman-Monteith equation given by Eq. (1) by considering the case where the energy supply is negligible:

$$PET = \frac{1}{L[T(z)]}\left[\frac{\rho_a \cdot c_p \cdot p_{v0}(z)[1-RH\ ]}{[\Delta \cdot r_a + \gamma\ (r_a + r_c)]}\right] \quad (5)$$

For the case where the air velocity is very low, the aerodynamic resistance r_a becomes very high as shown by Eq. (2). The aerodynamic resistance is then much greater than the canopy resistance and dominates the evaporation/evapotranspiration process. As a result, flow rate appears to be essentially the same for the bare and vegetated surfaces.

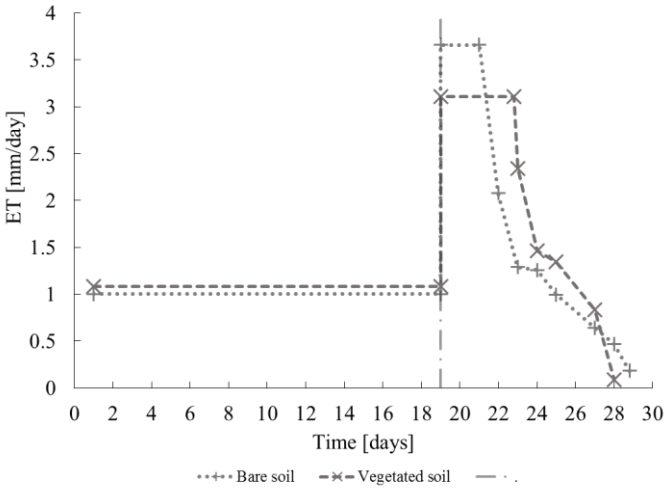

Figure 4. Evaporation/Evapo-transpiration rate for vegetated and bare soil

As soon as ventilation is imposed (onset of BC2 on Day 19), flow rate significantly increases as expected. This is consistent with Eq. (2) as an increase in wind velocity decreases the aerodynamic resistance r_a and, hence, generates an increase in the evaporation/evapotranspiration rate.

It can be noticed that flow rate is higher for the bare surface compared to the vegetated surface (Table 5). This can be explained by the reduction in aerodynamic resistance r_a, whose order of magnitude now becomes comparable to the canopy resistance r_c. The additional canopy resistance term r_c, which is only present for the vegetated cover, then generates a lower evapotranspiration rate for the vegetated cover compared to the bare soil.

Table 5. Potential evaporation/evapo-transpiration rates

Stage	BC 1	BC 2
$ET_{\text{Vegetated soil}}$ [mm/day]	1.08	3.11
$ET_{\text{Bare soil}}$ [mm/day]	1.00	3.66

After an initial stage where flow rate remains relatively high for both bare and vegetated surfaces, the flow rate starts to decline significantly as shown in Figure 4 (on Day 21 for the bare surface and on Day 23 for the vegetated surface). The hydraulic system enters the water-limited regime because it is no longer able to accommodate the evaporative demand of the environment (AET<PET).

Figure 4 shows that this condition is attained first by the bare surface. This is because water extraction is concentrated at the surface for the case of bare soil. To accommodate the water flux, high pore-water pressure gradients need to be generated in proximity of the surface, i.e. pore-water pressure is depleted significantly in the proximity of the evaporative surface. In turn, this causes a decrease in hydraulic conductivity of the top layers, which adds significant resistance to water flow.

On the contrary, water extraction is distributed along the entire root depth for the case of vegetated soil. Lower gradients are therefore required to accommodate water flow and pore-water pressure can remain relatively high in the root zone. The top layers in the vegetated soil remain more conductive than the top layers in the bare soil resulting in a higher AET for the vegetated soil in the water-limited regime.

This pattern is corroborated by the measurement of pore-water pressure and water content. Figure 5 and Figure 6 report the evolution over time of the profiles of volumetric water content (from TDRs measurement) and negative pore-water pressure (from HCTs measurements) for the two columns.

During the stage of natural ventilation (BC1), the pore-water pressure and water content profiles remain similar for the bare and vegetated soil (from Day 1 to Day 19) and this is consistent with the similar flow rate measured in the two columns.

When the samples enter the water-limited regime, it can be seen clearly that water content is depleted more in the vegetated sample compared with the bare sample (Figure 5). At the same time, the lower pore-water pressure (higher suction) developing in the bare soil close to the surface confirms that water extraction concentrated at the sample surface generates higher gradients in proximity of the surface.

It should also be noticed that the shape of the water content and pore-water profiles show gradients consistent with an outward flow (water content and pore-water pressures lower in proximity of the surface). This demonstrates the good quality of the monitoring system implemented in the columns.

At the end of the test water content was measured taking soil samples in the proximity of each TDR probe. The comparison between these values and the one from TDR probes, calculated using Ledieu are compared in Table 6. The error is very small, this demonstrates the good quality of the TDR measurement including the use if the Ledieu calibration curve.

Table 6. Comparison of volumetric water content measured by TDR and oven-drying

	Probe	θ_{Ledieu}	$\theta_{measured}$	$\Delta\theta$
Vegetated Column	TDR 1	0.013	0.0277	0.014
	TDR 2	0.033	0.0411	0.008
	TDR 3	0.046	0.0432	-
Bare Column	TDR 6	0.022	0.0263	0.004
	TDR 7	0.054	0.0481	-
	TDR 8	0.054	0.0498	-

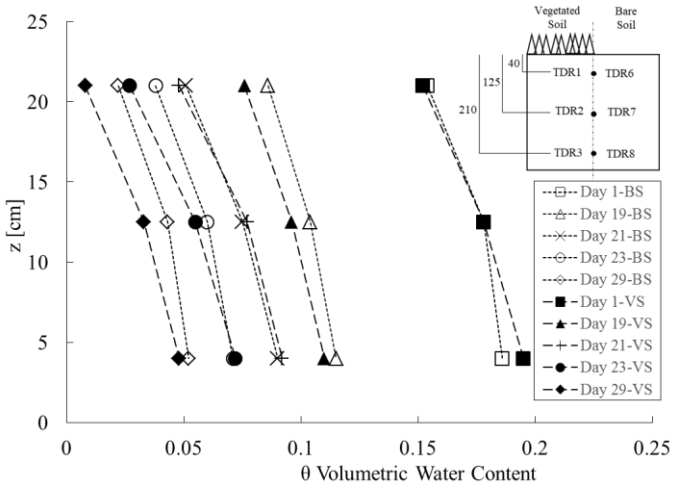

Figure 5. Evolution of volumetric water content profile over time, for vegetated and bare soil.

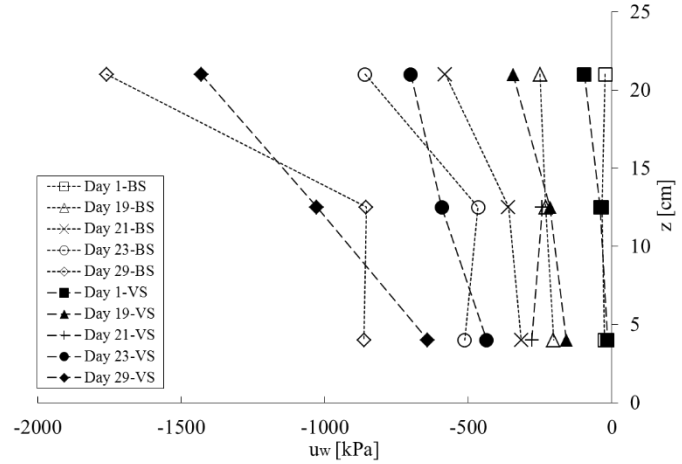

Figure 6. Evolution of the suction profile over time, for vegetated and bare soil.

5 CONCLUSIONS

The paper has presented an infiltration column to investigate the response of the Soil-Plant-Continuum-Atmosphere. The experimental setup was able to capture the change in evapotranspiration regime associated with the transition from natural to forced ventilation, i.e. the transition from the energy-limited to the water–limited regime. The profiles of

water content and suction recorded by TDR probes and the high-capacity tensiometers were coherent with the different stages in the evapotranspiration process. The response of the TDR probes has also been successfully validated by comparison with measurements of water content by oven-drying.

6 ACKNOWLEDGEMENTS

The authors wish to acknowledge the support of the European Commission via the Marie Skłodowska-Curie Innovative Training Networks (ITN-ETN) project TERRE 'Training Engineers and Researchers to Rethink geotechnical Engineering for a low carbon future' (H2020-MSCA-ITN-2015-675762).

7 REFERENCES

Ahrens, C.D., 2006. Meteorology Today: Introduction to Weather Climate and Environment, 2008. *Brooks/Cole, Belmont, California, US.*

Allen, R.G., Pereira, L.S., Raes, D. and Smith, M., 1998. Crop evapotranspiration-Guidelines for computing crop water requirements-FAO Irrigation and drainage paper 56. *FAO, Rome*, 300(9), p.D05109.

Fredlund, D.G., Morgenstern, N.R. and Widger, R.A., 1978. The shear strength of unsaturated soils. *Canadian geotechnical journal*, 15(3), pp.313-321.

Garg, A., Coo, J.L. and Ng, C.W.W., 2015. Field study on influence of root characteristics on soil suction distribution in slopes vegetated with *Cynodon dactylon* and *Schefflera heptaphylla*. *Earth Surface Processes and Landforms*, *40*(12), pp.1631-1643.

Kamchoom, V., Leung, A.K. and Ng, C.W.W., 2014. Effects of root geometry and transpiration on pull-out resistance. *Geotechnique Letters*, 4(1), pp.330-336.

Ledieu, J., De Ridder, P., De Clerck, P. and Dautrebande, S., 1986. A method of measuring soil moisture by time-domain reflectometry. *Journal of Hydrology*, 88(3-4), pp.319-328.

Monteith, J.L., 1965, July. Evaporation and environment. *In Symp. Soc. Exp. Biol* (Vol. 19, No. 205-23, p. 4).

Ng, C.W. and Menzies, B., 2007. *Advanced unsaturated soil mechanics and engineering*. CRC Press.

Penman, H.L., 1948. Natural evaporation from open water, bare soil and grass. *Proceedings of the Royal Society of London A: Mathematical, Physical and Engineering Sciences* (Vol. 193, No. 1032, pp. 120-145).

Penman, H.L. 1956. Evaporation: an introductory survey. *Netherl. J. Agric. Sci*. 4: 9-29.

Philip, J.R., 1966. Plant water relations: some physical aspects. *Annual Review of Plant Physiology*, 17(1), pp.245-268.

Pollen-Bankhead, N. and Simon, A., 2010. Hydrologic and hydraulic effects of riparian root networks on streambank stability: Is mechanical root-reinforcement the whole story?. *Geomorphology*, 116(3), pp.353-362.

Prescott, J.A., 1940. Evaporation from a water surface in relation to solar radiation. *Transactions of the Royal Society of South Australia*, 64(1), pp.114-118.

Simon, A. and Collison, A.J., 2002. Quantifying the mechanical and hydrologic effects of riparian vegetation on streambank stability. *Earth Surface Processes and Landforms*, 27(5), pp.527-546.

Tarantino, A. and Mongiovi, L., 2001. Experimental procedures and cavitation mechanisms in tensiometer measurements. *Geotechnical and Geological Engineering*, 19(3-4), pp.189-210.

Tarantino, A., Ridley, A.M. and Toll, D.G., 2008. Field measurement of suction, water content, and water permeability. *Geotechnical and Geological Engineering*, 26(6), pp.751-782.